Polystyrene Nanocomposite Materials by *In Situ* Polymerization into Montmorillonite–Vinyl Monomer Interlayers

Ahmed Akelah, Ahmed Rehab, Tarek Agag, Mohamed Betiha

Chemistry Department, Faculty of Science, University of Tanta, 31527 Tanta, Egypt

ABSTRACT: A different series of new polystyrene–clay nanocomposites have been prepared by grafting polymerization of styrene with vinyl-montmorillonite (MMT) clay. The synthesis was achieved through two steps. The first step is the modification of clay with the vinyl monomers, such as *N,N*-dimethyl-*n*-octadecyl-4-vinylbenzyl-ammonium chloride, *n*-octadecyl-4-vinylbenzyl-ammonium chloride, triphenyl-4-vinylbenzyl-phosphonium chloride, and tri-*n*-butyl-4-vinylbenzyl-phosphonium chloride. The second step is the polymerization of styrene with different ratios of vinyl-MMT clay. The materials produced were characterized by different physical and chemical methods: (1) IR spectra, confirming the intercalation of the vinyl-cation within the clay interlayers; (2) thermogravimetric analysis (TGA), showing higher thermal stability for PS–nanocomposites than polystyrene (PS) and higher thermal stability of nanocomposites with of phosphonium moieties than nanocomposites with ammonium moieties; (3) swelling measurements in different organic solvents, showing that the swelling degree in hydrophobic solvents increases as the clay ratio decreases; (4) X-ray diffraction (XRD), illustrating that the nanocomposites were exfoliated at up to a 25 wt % of organoclay content; and (5) scanning electron microscopy (SEM), showing a complete dispersion of PS into clay galleries. Also, transmission electron microscopy (TEM) showed nanosize spherical particles of ∼ 150–400 nm appearing in the images. © 2006 Wiley Periodicals, Inc. J Appl Polym Sci 103: 3739–3750, 2007

Key words: polymer–clay nanocomposites; polystyrene–nanocomposites; polystyrene–montmorillonite nanocomposites; intercalated polystyrene, polymer–clay hybrids

INTRODUCTION

Polymer–clay nanocomposites (PCNs) have attracted considerable attention because of their potential applications in industry.[1–4] These materials have been widely used in areas of electronics, transportation, and construction products. They offer attractive combinations of stiffness and toughness, which are difficult to attain from the individual component alone.[5] A nanocomposite is defined as a composite in which the dispersed particle size is $< 10^2$ nm in at least one dimension. Montmorillonite (MMT) is commonly used as a layered silicate clay in PCNs. PCNs are divided into intercalated and exfoliated hybrids. Intercalated hybrids retain registry between the host galleries with an expanded gallery distance. Exfoliated hybrids retain little or no registry between the silicate layers, which are separated by as much as 5–15 nm.[6] PCN have been prepared by four techniques: exfoliation adsorption,[7] *in situ* intercalative polymerization,[8] melt intercalation,[9,10] and template synthesis.[11]

Compared with pristine polymers, the PCNs possess many desirable properties, such as enhanced gas barrier; fire retardant, corrosion resistance, and ionic conductivity; increased thermal stability and mechanical strength; and decreased absorption in organic liquids.[12,13] Because the nanostructures of nanocomposites are essentially related to their properties, a number of fundamental studies have been performed and have revealed some parameters affecting the nanostructures, such as the molecular weight and polarity of polymers[9] and chain length, packing density, and arrangement of organic modifiers.[9,14]

The impregnation of a clay by a vinyl monomer, such as methyl methacrylate,[15] acrylonitrile,[16] oligo (oxyethylene) methacrylate,[17] or styrene,[18–22] followed by free radical polymerization, has recently been investigated.

Several attempts to prepare intercalated polystyrene–clay nanocomposites, different microstructures, according to the type of organic modifier and polarity of the polymer matrix, have been reported.[18–21,23,24] Kato et al.[18] reported that the intercalation of polystyrene in stearyltrimethylammonium cation exchanged MMT. Other investigators have prepared intercalated polystyrene nanocomposites using acetonitrile as a solvent in which the vinylbenzyltrimethylammonium ions were exchanged with the sodium

ions of MMT.[19,20] Doh and Cho[22] reported the synthesis of intercalated polystyrene containing dispersed organophilic MMT.

The modifications of clay with a specific monomers or polymers improve the interfacial properties between the organic and inorganic phases of the nanocomposites. Therefore, in the present investigation, the intercalation of vinyl monomeric cations onto MMT clay; using *N,N*-dimethyl-*n*-octadecyl-4-vinylbenzyl-ammonium chloride, *n*-octadecyl-4-vinylbenzyl-ammonium chloride, triphenyl-4-vinylbenzyl-phosphonium chloride, and tri-*n*-butyl-4-vinylbenzyl-phosphonium chloride; will be prepared. The resulting vinyl–clay intercalate is directed toward the preparation and characterization of grafted polystyrene–clay nanocomposites that can exhibit the characteristic properties of the individual components. This can be attained by in situ free radical polymerization techniques of styrene monomer between the smectic clay interlayers.

EXPERIMENTAL

Materials

Chloromethylstyrene (CMS) [vinyl benzyl chloride] was obtained from Polyscience as a mixture of *m/p*-isomers ($\cong$ 30/60) and was used as supplied. Styrene (St) is commercial supplied from Aldrich, used after discharge the inhibitor by washing with $1M$ NaOH solution then dried over Na_2SO_4, followed by distillation under vacuum. 2,2-Azobisisobutyronitrile (AIBN) was obtained from Fluka (Switzerland) and used without further purification. *n*-Octadecylamine and *N,N*-dimethyl-*n*-octadecylamine were purchased from Kunimine Industry (Japan) and used as supplied without further purification. Triphenylphosphine and tributylphosphine were used as received from Fluka. Sodium MMT clay (Na^+–O–MMT) with a cation-exchange capacity (CEC) of $\sim$ 119 mEq per 100 g was supplied by Kunimine Industry under the trade name Kunipia-F. Dimethylformamide (DMF) and toluene were obtained from Adwic (Egypt) and were used after distillation and drying over an A4 molecular sieve directly before used. Ethanol, methanol, and diethyl ether were used as obtained from Adwic without further purification.

Analytical procedures

Infrared spectra (IR) were carried out on a Perkin-Elmer 1430 Ratio-recording infrared spectrophotometer, using the potassium bromide disc technique within the wavenumber range of 4000–400 cm^{-1}.

^{1}H-NMR and ^{13}C-NMR spectra were carried out in CDCl$_3$ on an Lambda, Jeol NM300, Japan Instrument. Thermogravimetric analyses (TGA) were determined with Rigaku Thermo Plus 2 TG-DTA TG8120. The

heating rate was 5–10°C/min under air and argon atmosphere within the temperature range $\sim$ 30–900°C.

Calcination was determined by introducing a definite weight of the sample into a porcelain crucible and dried in an electric oven at 120°C overnight, then introduced into an ignition oven; the temperature was increased to 1000°C and was adjusted for 5 h at this temperature. The loading of each sample expressed as the weight loss by ignition per 100 g of the dry sample.

The swelling degree was determined by taking a definite weight ($\sim$ 0.15 g) of the dry sample and introduced into a small sintered glass and allowed to imbibe for 24 h in different solvents. The excess solvent was removed by gentle centrifugation. The swelled sample was weighed and resuspended in the solvent. This procedure was repeated until obtaining on a constant weight for the swelled sample. The swelling degree of each sample is expressed as the amount of sorbed solvent per 100 g of dry sample.

X-ray diffraction (XRD) measurements were carried out using a Phillips Powder-Diffractometer equipped with Ni-filtered Cu-K radiation ($\lambda = 1.5418$ Å) at a scanning rate of 0.005°/s, diverge at slit 0.3°. Measurements were made for the dried product to examine the interlayer activity in the composite as prepared.

The morphology of the composite was examined by two techniques: (1) scanning electron microscopy (SEM) Joel JXA-840 equipped with an energy-dispersive X-ray detector to examine the morphology and particle size of MMT in the polymer-MMT composites, with the specimen deposited on double-sided scotch tape and examined at their surface; and (2) transmission electron microscopy (TEM) images of the composites, obtained by a Joel 100 CX at 80 kV; the thin films for TEM were prepared by immersing the TEM grid in suspension of polymer–clay material swelled in acetone, and then dried at room temperature followed by heating at 50°C under vacuum to ensure complete solvent removal.

Preparation of vinyl monomer (I$_{a-d}$)[25]

Synthesis of triphenyl(4-vinylbenzyl) phosphonium chloride salt I$_a$

A mixture of vinyl benzyl chloride (5.8 g, 38 mmol), triphenylphosphine (10.0 g, 38 mmol), and 0.03 g of hydroquinone as the free radical inhibitor was dissolved in 60 mL of dry DMF in a round-bottom flask. The solution mixture was stirred at 60°C for 6 h and was then poured into 400 mL of diethyl ether with stirring; the stirring continued for 30 min. The precipitated product was filtered off then recrystallized from diethyl ether/methanol (1 : 5 v/v), to give 12.5 g (30 mmol, 79% yield) of triphenyl(4-vinylbenzyl) phosphonium chloride I$_a$.

^{1}H NMR (CDCl$_3$): δ = 7.65–6.92 (*m*, 19 H, ring H), 6.48 (*dd*, 1H, vinyl H), 5.55 (*d*, 1H, vinyl H), 5.28 (*d*, 2H, Ph—CH$_2$), and 5.7 ppm (*d*, 1H, vinyl H).

^{13}C-NMR (CDCl$_3$): δ = 137.2 (=CH$_2$), 137.25, 135.73, 134.78, 134.17, 134.03, 133.58, 133.32, 131.88, 131.81, 131.77, 131.75, 131.49, 131.42, 130.01, 129.85, 128.52, 128.3, 128.22, 126.28, 126.23, 118.1, 115.97 (Ar), 114.55 (Ar—CH=) and 30.76 ppm (P—CH$_2$).

IR (KBr disc): ν = 1432, 1157, and 1039 cm^{-1} for $^+$P(Ph)$_3$ and at 1614 cm^{-1} for (—C=C—).

Formation of tri-*n*-butyl(4-vinylbenzyl) phosphonium chloride salt I$_b$

This phosphonium salt, **I$_b$** was prepared by similar procedure described in preparation of **I$_a$**, by mixing of 3.8 g (24.7 mmol) of vinyl benzyl chloride with 5.0 g (24.7 mmol) of tri-*n*-butylphosphine in presence of 0.02 g of hydroquinone in 50 mL of dry DMF. The solution mixture was stirred at room temperature for 1 h and then poured into an excess of diethyl ether with stirring. The precipitated product was filtered off, washed with diethyl ether, and finally dried in vacuum at room temperature (∼ 30°C), to give 7.5 g of salt **I$_b$**, which corresponds to 85% of the product yield.

^{1}H NMR (CDCl$_3$): δ = 7.29–7.21 (*m*, 4H, ring H), 6.54 (*dd*, 1H, vinyl H), 5.63 (*s*, 1H, vinyl H), 5.15 (*s*, 1H, vinyl H), 4.17 (*s*, 2H, Ph—CH$_2$), 2.27 (*s*, 6H, PhCH$_2$), 1.32 (*s*, 12H, CH$_2$CH$_2$), and 0.76 ppm (*s*, 9H, CH$_2$CH$_3$).

^{13}C-NMR (CDCl$_3$): δ = 137.28(C—Ar), 135.55 (Ar—CH=), 130.1, 127.87, 127.75, 126.72 (C—Ar), 114.58 (=CH$_2$), 26.74, 26.15, 23.78, 23.58, 23.42, 18.65, 18.03, and 13.159 ppm ((—CH$_2$).

IR (KBr disc): ν = 1457, 1211 and 1098 cm^{-1} for $^+$P(Bu)$_3$ and at 1605 cm^{-1} for (—C=C—).

Synthesis of *n*-octadecyl(4-vinylbenzyl) ammonium chloride salt I$_c$

In a round-bottom flask, 10.0 g (37 mmol) of stearylamine was dissolved in 50 mL of dry DMF, followed by the addition of 0.03 g of hydroquinone; 6.5 g (37 mmol) of vinyl benzyl chloride was added dropwise in a period of 4 h to the stirred solution at 45°C. After cooling, the reaction solution mixture was added dropwise with stirring to an excess of diethyl ether. The white precipitated product was filtered off, washed with diethyl ether, and then dried in vacuum at room temperature, to give 12.8 g of salt **I$_c$** with 82% product yield.

^{1}H-NMR (CDCl$_3$): δ = 9.81 (*s*, 2H, $^+$NH$_2$), 7.51–7.37 (*m*, 4H, ring H), 6.63 (*dd*, 1H, CH=), 5.7 (*d*, 1H, —CH=), 5.24 (*d*, 1H, —CH=), 3.98 (*s*, 2H, Ph—CH$_2$), 2.98–1.18 (*m*, 34H, CH$_2$CH$_2$), and 0.85 (*m*, 3H, CH$_3$).

^{13}C-NMR (CDCl$_3$): δ = 138.67 (Ar), 135.89 (=CH), 130.60, 129.40, 126.81 (Ar), 115.18 (—CH=), 50.09 (Ar—CH$_2$), 45.91 (NH$_2$—CH$_2$), 39.99, 31.94, 31.90,

31.87, 29.68, 29.58, 29.50, 29.41, 29.33, 29.00, 27.63, 26.77, 25.83, 22.06 (17CH$_2$), and 14.08 ppm (1CH$_3$).

IR (KBr disc): ν = 3403 cm^{-1} for N—H stretching, 2688 cm^{-1} for—NH$_3$ bending and at 1605 cm^{-1} for (—C=C—).

Synthesis of *N,N*-dimethyl-*n*-octadecyl(4-vinylbenzyl) ammonium chloride salt I$_d$

The ammonium salt, **I$_d$** was prepared by similar procedure as described in preparation of **I$_c$**, by mixing 10.0 g (34.36 mmol) of *N,N*-dimethyl-*n*-octadecylamine dissolved 10 mL THF and 5.24 g (34.36 mmol) of vinyl benzyl chloride **I$_d$**. The mixture was stirred 2 h at room temperature then diethyl ether (200 mL) was added, and the mixture was stirred for another 1 h. The precipitated product was filtered off, and recrystallized from ethyl acetate at 45°C, to give 13.8 g of **I$_d$** (yield = 91%). The characteristic data correspond to those reported previously.[10]

Preparation of vinyl monomer–clay II$_{a-d}$[25]

Preparation of the phosphonium salt-modified clay II$_{a,b}$

A suspension of 10 g (11.9 mEq) of sodium MMT in 300 mL of distilled water was stirred for 24 h in an Erlenmeyer flask to complete swelling. Then, ∼ 30 mL of methanol was added dropwise with stirring, and the stirring was continued for 2 h. To the stirred swelled clay suspension, a solution of 5.0 g (11.9 mmol) **I$_a$** in 100 mL of distilled water was added dropwise. After stirring for 4 h, the white precipitate product was filtered, washed with distilled water several times until no chloride ion could be detected by an addition of AgNO$_3$ solution to the filtrate, and then washed twice with 80 : 20 (v/v) ethanol/water. The white powder product was dried in a vacuum oven overnight at room temperature, to give 12.85 g of **II$_a$**.

XRD data: 2θ = 3.82°, d-spacing = 23.12 Å.

Calcination data: inorganic contents = 70.4 (wt %); organic contents = 29.6 (wt %).

The same procedure was used to produce 12.2 g of **II$_b$** by addition of 4.22 g (11.9 mmol) **I$_b$** to 10 g of swelled clay.

XRD data: 2θ = 4.83°; *d*-spacing = 18.29 Å.

Calcination data: inorganic contents = 66.35 (wt %); organic contents = 33.65 (wt %).

Preparation of the ammonium salt-modified clay II$_{c,d}$

The ammonium salt-modified clay **II$_c$** and **II$_d$** were prepared carrying the same procedure used in the preparation of **II$_a$**.

The vinyl–clay **II$_c$** was synthesized by dropwise addition a solution of 5 g (11.9 mmol) ammonium

TABLE I
Preparation Data for Polystyrene–Organoclay Hybrids

Run	Monomer–clay		Solvent		St (g)	Product				
	Type	Wt (g)	Type	ML		Grafted	Ungrafted		Calcination (%)	
							(g)	(η_{rel})	Inorg	Organic
$III_{a(1)}$	II_a	0.1	9.9	Tol	5	0.15	6.4	1.1714	50	50
$III_{a(2)}$	II_a	0.5	9.5	Tol	20	0.67	2.7	1.1429	62	38
$III_{a(3)}$	II_a	0.5	9.5	Tol + Diox	20 + 5	0.71	2.1	1.2000	37	63
$III_{a(4)}$	II_a	1.0	9.0	Tol	40	1.34	0.12	1.2000	61.33	38.67
$III_{a(5)}$	II_a	2.5	7.5	Tol	70	3.1	0.44	1.1524	66.91	33.09
$III_{b(1)}$	II_b	0.1	9.9	Tol	5	0.14	6.5	1.2857	39.21	60.79
$III_{b(2)}$	II_b	0.5	9.5	Tol	10	1.03	5.5	1.1619	44.8	55.2
$III_{b(3)}$	II_b	0.5	9.5	MeCN	2	1.3	4.42	1.1619	37.56	62.44
$III_{b(4)}$	II_b	1.0	9.0	Tol	20	2.19	5.52	—	45.64	54.36
$III_{b(5)}$	II_b	1.0	9.0	MeCN	4	1.26	5.0	1.2095	22	78
$III_{b(6)}$	II_b	2.5	7.5	Tol	50	4.34	0.5	1.1429	59.64	40.36
$III_{c(1)}$	II_c	0.1	9.9	Tol	5	0.3	6.53	1.2190	13.62	86.38
$III_{c(2)}$	II_c	0.5	9.5	Tol	15	0.72	6.12	—	52.54	47.46
$III_{c(3)}$	II_c	0.5	9.5	—	—	—		—	3.4	96.6
$III_{c(4)}$	II_c	1.0	9.0	Tol	45	1.46	2.0	1.1429	55	45
$III_{c(5)}$	II_c	2.5	7.5	Tol	50	3.43	0.42	1.1619	55	45
$III_{d(1)}$	II_d	0.5	9.5	Tol	3	9.1		—	2.8	97.2
$III_{d(2)}$	II_d	1.0	9.0	Tol	6	8.7		—	5.8	94.2
$III_{d(3)}$	II_d	2.0	8.0	Tol	15	8.0		—	10.3	89.7
$III_{d(4)}$	II_d	4.0	6.0	Tol	50	7.8		—	21	79

Grafted = insoluble part obtained after washing with Soxhlet; ungrafted = soluble part on washing in toluene with Soxhlet.

salts I_c dissolved in 100 mL of water/methanol [70 : 30 v/v] to 10 g of swelled clay followed by stirring for 8 h, to give 12.8 g of II_c.

XRD data: 2θ = 3.83°, and 7.1°; d-spacing = 23 Å, and 12.4 Å.

Calcination data: inorganic contents = 56.57 (wt %); organic contents = 43.43 (wt %).

The synthesis of vinyl–clay II_d was carried out by addition dropwise a solution of 5.27 g (11.9 mmol) ammonium salts I_d dissolved in 100 mL of water/ methanol [70 : 30 v/v] to 10 g of swelled clay followed by stirring for 8 h, to give 13.9 g of the product II_d.

XRD data: 2θ = 2.63°, 4.78°, and 7.2°; d-spacing = 33.6 Å and 18.48 Å, and 12.4 Å.

Calcination data: inorganic contents = 50.76 (wt %); organic contents = 49.24 (wt %).

Preparation of PS–organoclay nanocomposites III_{a-d}

General procedure

In a 50-mL round flask, 0.1 g of organically modified clay was swelled in 5 mL dry toluene; 9.9 g of styrene monomer was then added, followed by the addition of 0.1 g of AIBN as a radical initiator, and then stirred at room temperature ($\sim$ 2–3 h) to obtain a swelled suspension. The mixture was heated in oil bath at $\sim$ 80°C for 2 h. After cooling, the product was precipitated in methanol. The precipitated PS–MMT hybrid was filtered, washed with methanol, and finally dried under reduced pressure for 24 h at 60°C, to give $III_{a(1)}$. The different composite mixtures were prepared following the same procedure, and the relevant data are illustrated in Table I.

RESULTS AND DISCUSSION

Preparation

The chemical grafting of polystyrene into clay interlayers by polymerization was achieved through three steps as illustrated in Schemes 1 and 2. The first step includes the preparation of monomeric surfactants such as triphenyl(4-vinylbenzyl) phosphonium chloride salt I_a, tri-n-butyl(4-vinylbenzyl) phosphonium chloride salt I_b, n-octadecyl(4-vinylbenzyl) ammonium chloride salt I_c and N,N-dimethyl-n-octadecyl (4-vinylbenzyl) ammonium chloride salt I_d. The second step includes the preparation of vinyl monomer–clay intercalates, by cation exchange between the onium groups of vinyl monomer, forming an ionic bond with the negative charges of MMT clay interlayers. The third step includes complete dispersion of vinyl monomer–clay (with different ratios; 1, 5, 10, 25, and 40 wt %) in the styrene monomer, followed by free-radical polymerization to produce the PS–clay intercalated or/and exfoliated nanocomposites. The relevant polymerization condition data for the different series of polystyrene–clay materials were recorded in Table I.
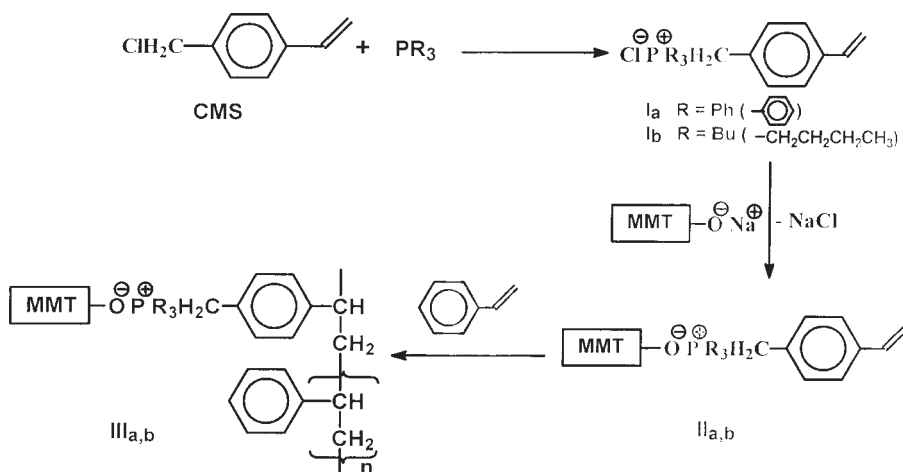
Scheme 1 Preparation of triphenyl and tributyl(4-vinylbenzyl) phosphonium salt–clay and its polymerization with styrene.

The ungrafted PS was separated by extraction with toluene, as a good solvent for polystyrene, using the soxhlet technique. The separated ungrafted PS with relative viscosity (0.05 g in 10 mL DMF at room temperature) ranged from 1.1429 to 1.2857. It was found that there are many samples can not be separate the ungrafted (if present), as these samples form a semi-clear solutions. This indicates that the clay was distributed homogeneously and highly exfoliated in PS matrix forming organic–inorganic species. The type of the onium salt group in vinyl monomer–clay has affected the properties of the produced composite product, since the salts of vinyl surfactants II_c and II_d leads to high, fast swelling in styrene monomer than do vinyl salts II_a and II_b. Also, the structure of the ammonium salt group has affected the properties of the composite, since the composites of the disubstituted amine surfactant, III_d, showed higher swelling and semi-clear solu-

tions in styrene than the composites of unsubstituted amine surfactant, III_c. Thus, the bulk polymerization of styrene in the vinyl–clay interlayers leads to highly dispersed and exfoliated clay into PS matrix. For example, in the sample $III_{c(3)}$, the organoclay II_c highly swelled in styrene monomer without solvent, and free radical polymerized, to give highly suspended product (semi clear solution) in toluene.

The clay content as shown in Table I has also affected the polymerization process, since the amount of ungrafted PS decreases with increased clay content. This may be duo to the isothermal character of MMT, which prevent the complete polymerization process, since MMT act as chain transfer terminator,[13] rather than the solvent used. However, the amount of grafted PS onto clay does not appear to be very different between the samples, in using different clay contents. Also, the data in the Table I show that the type of the solvent used in the prepa-
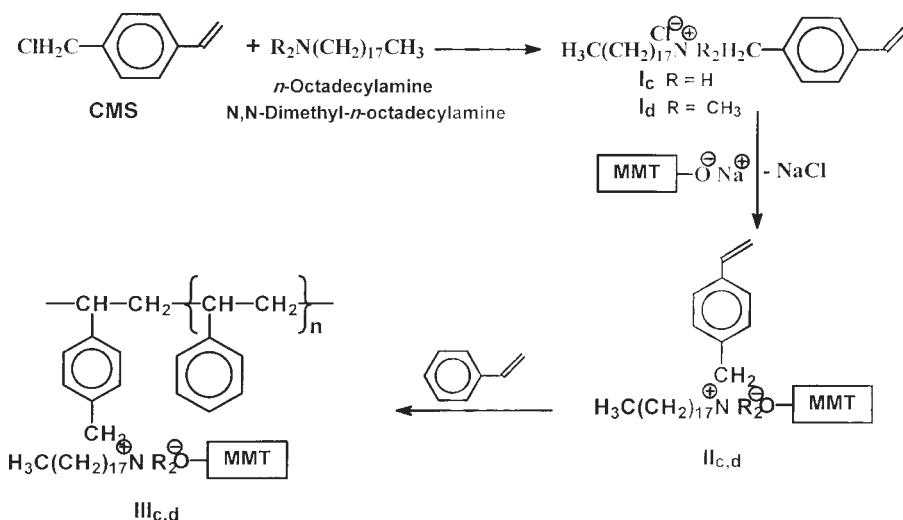
Scheme 2 Preparation of *n*-octadecyl and *N,N*-dimethyl-*n*-octadecyl (4-vinylbenzyl) ammonium salt–clay and its polymerization with styrene.

ration of PS–clay composites is an important factor affecting the grafted PS into clay interlayers. In sample $III_{a(3)}$, the use of mixed solvent (1,4-dioxane and toluene) leads to increased the grafted PS into clay interlayers. Also, in sample $III_{b(3)}$, the weight of grafted PS increased in case of using acetonitrile than toluene as solvents. The increasing in the grafted PS may be due to increasing the swelling degree of vinyl monomer–clay, which leads to increasing the amount of styrene monomer inside clay gallery before polymerization.

Properties and characterization

The prepared monomers were found to be soluble in toluene and in polar solvents such as water, alcohol, acetonitrile, DMF, and styrene monomer, but were found to be insoluble in the aliphatic hydrocarbons and diethyl ether.

Swelling studies

MMT is constructed from an octahedral silica sheets; it exhibits net negative charges on the lamellar surface attached by cations (Na^+). Thus, in this case where the interlayer is incorporated with sodium cation, the hydrophilic properties must be enhanced, which in turn leads to high degree of water swelling. Therefore, these phenomena can possibly provide an effective method for the preparation of hybrid composite intercalated or exfoliated with monomer or polymer in the layered silicate if an aqueous system is involved in the intercalation procedure or clay

surface become hydrophobic by exchange sodium cation by ammonium or phosphonium cation.

The swelling measurements of the organoclay and the grafted polymer onto clay in different solvents (e.g., DMF, 1,4-dioxan, acetone, toluene, chloroform, dichloromethane, and water) are listed in Table II, expressed as the percentage of sorbed solvent related to the dry weight of the sample. The data indicate that the hydrophilic character of the mineral clay has been changed into hydrophobic character, due to the intercalation of the vinyl monomers in the clay interlayers. In general, the swelling measurement data show that the hydrophobic characters of all prepared intercalated compounds were increased in the organic solvents, and there is great reduction in the water uptake capacities of grafted polymer clay. It was also found that the grafted PS–clay has great affinity for an aprotic solvent like dimethylformamide (DMF) and nonpolar solvent like toluene. The polar solvents show a lower degree of swelling, which can be attributed to the hydrophobic characteristics of PS, leading to the increased solubility in nonpolar solvents than in polar solvents. There is no regular order that can be followed from the swelling measurements.

NMR and IR measurements

The structures of the monomers were identified by using ^1H-NMR, ^{13}C-NMR, and IR. The ^1H-NMR data were recorded for vinyl monomers I_{a-d} in the experimental part, in which the H of chloromethyl group (CH_2Cl) was shifted from 4.6 ppm for CMS to 5.3 ppm corresponding to the quaternary salt for I_a,

TABLE II
Swelling Degrees Data for Different Vinyl Monomer–clay and Grafted Polystyrene–Clay Composites

Sample	Swelling (%)						
	DMF	Dioxane	Acetone	Toluene	CH_3Cl	CH_2Cl_2	H_2O
II_a	1158	394	190	219	312	190	—
II_b	955	224	701	228	226	155	—
II_c	365	250	143	262	152	187	—
$III_{a(1)}$	1242	906	557	697	481	1123	50
$III_{a(2)}$	1537	376	374	651	248	1291	85
$III_{a(3)}$	1172	373	315	664	361	1277	10
$III_{a(4)}$	1123	367	783	990	315	911	55
$III_{a(5)}$	1001	327	558	547	174	998	106
$III_{b(1)}$	984	459	26	601	10	32	32
$III_{b(2)}$	808	435	26	544	64	31	41
$III_{b(3)}$	900	400	115	700	110	70	50
$III_{b(4)}$	684	159	117	600	10	62	32
$III_{b(5)}$	750	390	140	650	60	65	40
$III_{b(6)}$	763	107	34	352	39	29	114
$III_{c(1)}$	1132	110	78	399	639	625	100
$III_{c(2)}$	744	133	56	392	513	268	92
$III_{c(3)}$	672	183	59	394	175	210	112
$III_{c(4)}$	298	157	17	299	153	88	46

4.17 ppm for I_b, and to 3.98 ppm for I_c. Also the peak at about 6 ppm corresponding to amine proton of stearylamine shifted to 9.8 ppm with integration of two protons corresponding to ($-N^+H_2$). The peaks at 5.0, 5.6, and 6.6 ppm revealed the presence of vinyl group. The absorption band of ^{13}C-NMR spectra corresponding to one carbon of chloromethyl group (CH_2Cl) at 46 ppm was shifted to 30 ppm, corresponding to the quaternary salt for I_a, 26 ppm for I_b and to 50 ppm for I_c.

The IR spectra of vinyl monomers and intercalated vinyl monomers onto MMT clay were studied to confirm the structural composition of the materials (Fig. 1). The spectra of vinyl monomers showed a characteristic band at 1614 cm^{-1} for I_a, 1630 cm^{-1} for I_b and 1605 cm^{-1} for I_c related to vinyl group (C=C), and band at 838 cm^{-1} related to C—Cl of the chloromethyl groups. The IR spectra of vinyl monomer–clay II_{a-d} show that the band at 838 cm^{-1} related to C—Cl of chloromethyl groups disappeared, as well as characteristic bands corresponding to the phosphonium salt, $P^\oplus$ (R)$_3$, at 3414 cm^{-1}, and the ammonium salt, $N^\oplus$ (R)$_3$, at 3433 cm^{-1}.

The IR spectrum of I_a shows characteristic bands at 1432 cm^{-1}, 1157 cm^{-1}, and at 1039 cm^{-1} related to the phosphonium salt attached to the Ph group. Comparison of these bands of phosphonium salt with the bands of II_a showed a shift from 1039 cm^{-1} to 916 cm^{-1} which indicated that the phosphonium salt must be interacted to metal oxide similar to the P—O band.

The IR spectrum of I_b shows characteristic bands at 1457, 1211, and 1098 cm^{-1} corresponding to phosphonium salt attached to the butyl group. These bands of phosphonium salt with II_b showed a shift to 911 cm^{-1} was reported, indicating that the phosphonium salt must be interacted to metal oxide similar to the P—O band. The broadness of this characteristic band is apparently related to intermolecular interaction.

The IR spectra of I_c display a characteristic band at 3600 cm^{-1} for the OH group, bands at 2649 cm^{-1}, 1794 cm^{-1} related to the protonated amine ($^+$NH) group, bands at 1499 cm^{-1} related to the ammonium salt itself, and bands at 1348 cm^{-1} related to C—N. The presence of extra peaks for modified clay is $\sim$ 2920 cm^{-1} and 2849 cm^{-1} for CH_2 and also $\sim$ 1831 cm^{-1} for the presence of $^+$NH group.

The characteristic bands of Na-MMT show the absorption bands at 1030 cm^{-1} and 550 cm^{-1} corresponding to the stretching band of Si—O, the deformation band of Si—O—Al and the Si—O—Si deformation band of MMT. These indicated that organic material stay immobilized inside and/or on the clay layers. IR spectra of the grafted PS–MMT composites illustrate the disappearance of absorption band of —C=C—.
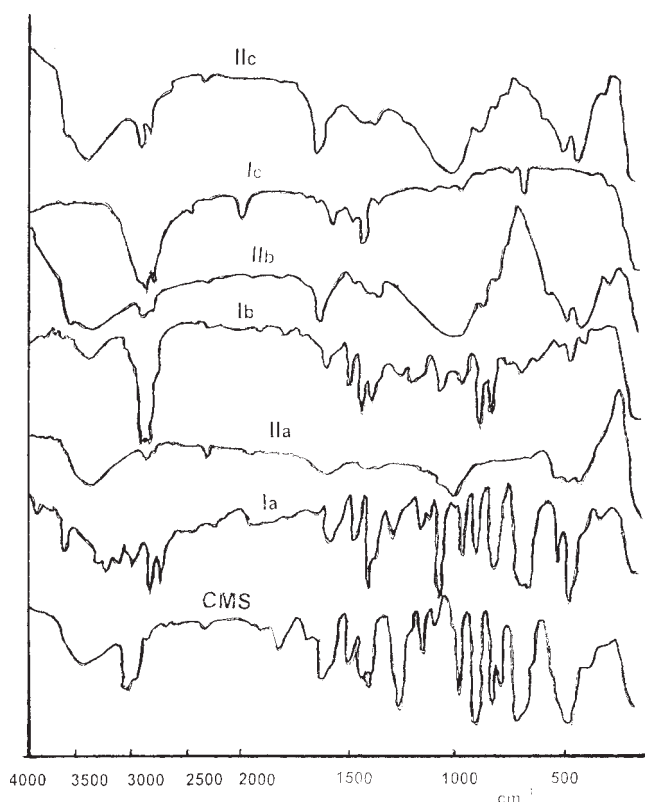
**Figure 1** IR spectra for CMS, vinyl monomer I_{a-c} and vinyl monomer–clay intercalate II_{a-c}.

XRD measurements

The crystal structure of MMT consists of two-dimensional layers formed by fusing two silica tetrahedral sheets to an edge-shared octahedral sheet of aluminum hydroxide. Stacking of layers of clay particles are held by weak dipolar or van der Waals forces.[26] XRD is powerful technique to observe the extent of the silicate dispersion ordered or disordered structure in the polymer nanocomposites. Figures 3–6 show typical XRD for the vinyl–clay and PS–MMT samples. The d_{001} spacing was calculated and listed in the experimental part from peak positions using Bragg's law of diffraction:

$$d = \lambda/(2\sin\theta),$$

where d is the space between interlayers; λ is the radiation wavelength of the of X-ray source; θ is the angle of incident radiation.

The XRD results for monomer-MMT are shown in the experimental part and Figure 2. The data in Figure 2 shows that the d-spacing of the intercalated monomers into MMT clay is affected by the molecular mass of the monomer, since d-spacing was increased from 1.2 nm ($2\theta = 7.2°$) for the Na-MMT
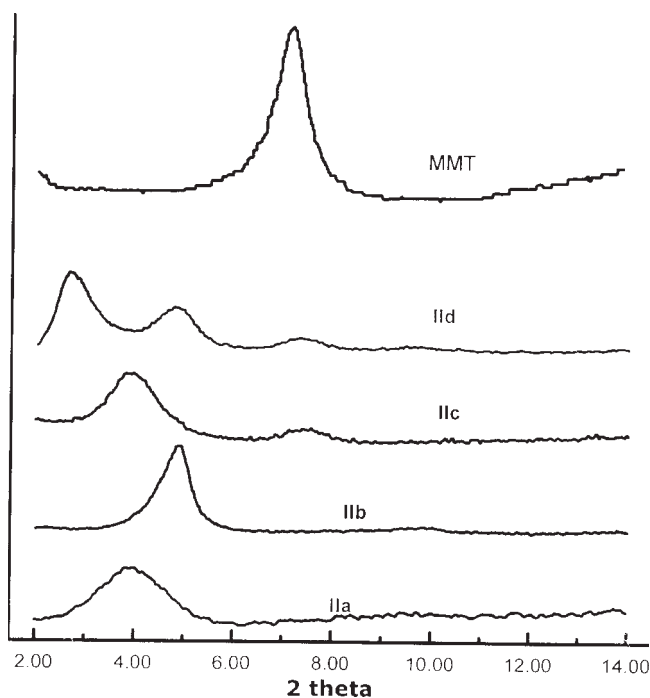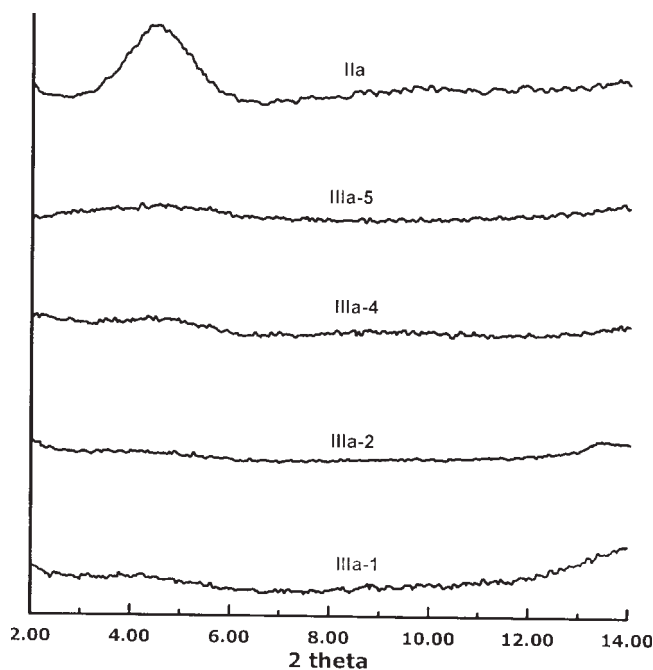
Figure 2 XRD for MMT clay and vinyl monomer–clay intercalates II_{a-d}.

Figure 3 XRD for vinyl monomer–clay intercalates II_a and grafted PS–clay materials III_a.

clay to 2.312 nm ($2\theta = 3.82°$) for II_a; 1.829 nm ($2\theta = 4.83°$) for II_b; 2.30 nm ($2\theta = 3.83°$) for II_c; and 3.36, 1.848 nm ($2\theta = 2.63°$, 4.78°) for II_d. The results revealed that the *d*-spacing in the order of $II_d > II_c \approx II_a > II_b$, coinciding with the order of the molecular weight of the monomers (450, 422, 414, 354). A small, broad peak at $2\theta = 7°$ was shown for the sample II_c, which may arise from incomplete exchange process of sodium ion in MMT by the ammonium ion of vinyl monomer modifier due to the hydrophobic nature of the salt. Also, there are two peak at $2\theta = 2.63°$ and 4.78° for the vinyl monomer–clay II_d. This may be due to the lack interlayers symmetrical arrangement of modified clay.

The XRD results for grafted polystyrene-MMT are shown in Figures 3–6 for the composites $III_{a(1–5)}$, $III_{b(1–6)}$, $III_{c(1–5)}$, and $III_{d(1–4)}$. Figures 3–6 show that there is no peak in all the PS–clay composites, except for a few samples. This indicated that the d_{001} reflection was shifted to lower diffraction-angle ($2\theta < 2°$) as a result of increasing the gallery height of the clay interlayers due to increasing the amount of polymer between lamella. Thus, the clay was homogeneously dispersed and exfoliated in the polymer matrix forming exfoliated nanocomposite materials.

Figure 5 shows that the nanocomposites $III_{c(5)}$ (25 wt % organoclay) has a broad peak at $2\theta = 4.7°$ with low intensity and a small broad peak at $2\theta = 7.1°$. Figure 6 shows that the sharp peak at $2\theta = 2.5°$ with high intensity in II_d was diminished, broadening to

$2\theta = 2.5–2.7°$. Also, in Figure 6, the sample $III_{d(4)}$ with high organoclay contents (40%) with the peak intensity at $2\theta = 4.7°$ disappeared. This can be explained as the unhomogeneously distributed polymer in the clay interlayers which leads to a little dispersion of the clay stacks in the styrene matrix. Also,
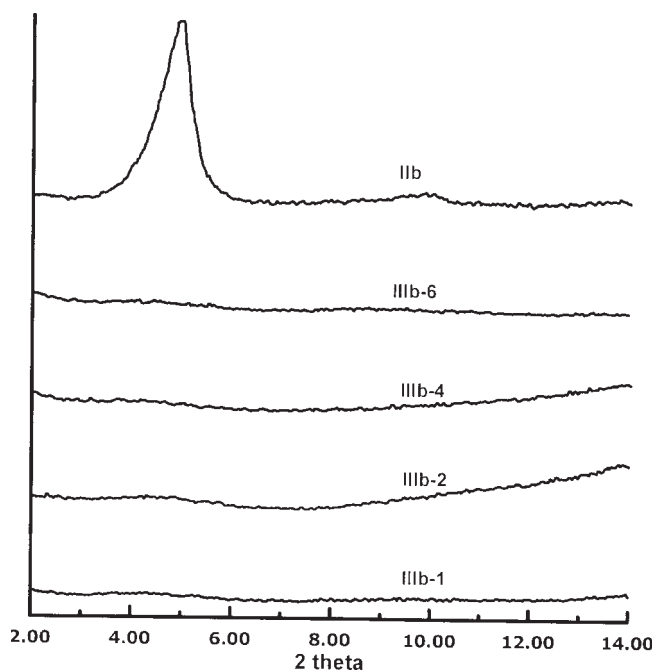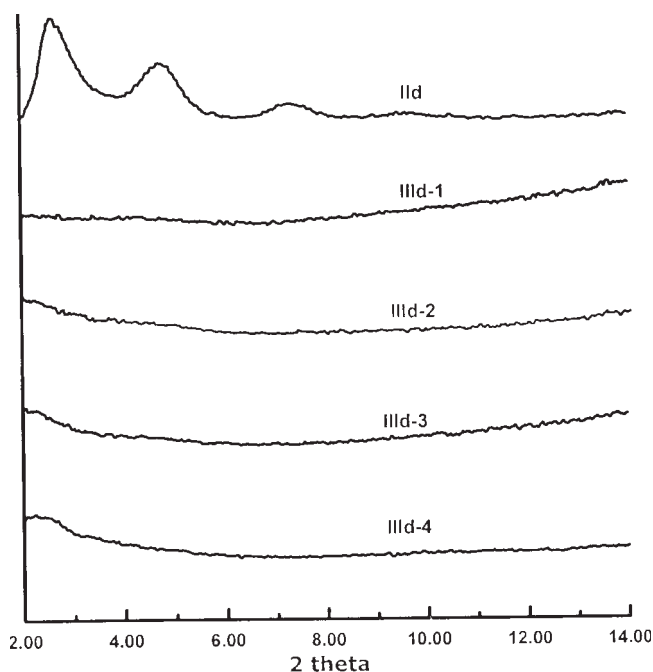

**Figure 4** XRD for vinyl monomer–clay intercalates II_b and grafted PS–clay materials III_b.
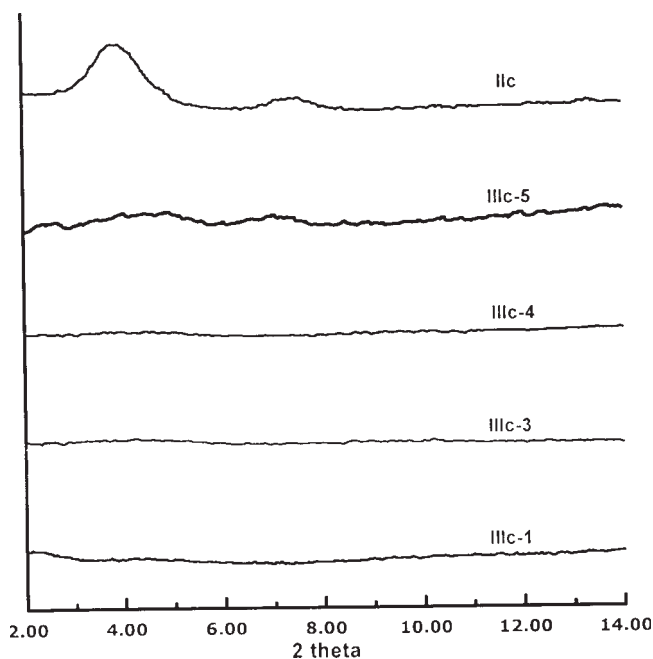
Figure 5 XRD for vinyl monomer–clay intercalates **II**c and grafted PS–clay materials **III**c.

it can be explained by the possibility of occurrence of a Hofmann elimination reaction to produce an olefin and amine,[27] according to the mechanism in Scheme 3, leaving a proton occupying the cationic position on the clay. It is well known that onium salts will participate in such a reaction,[28] and the thermal degradation of an ammonium counter ion in

Figure 6 XRD for vinyl monomer–clay intercalates **II**d and grafted PS–clay materials **III**d.
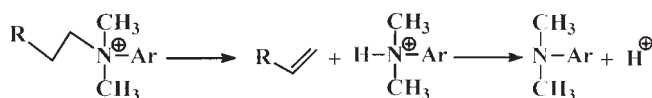
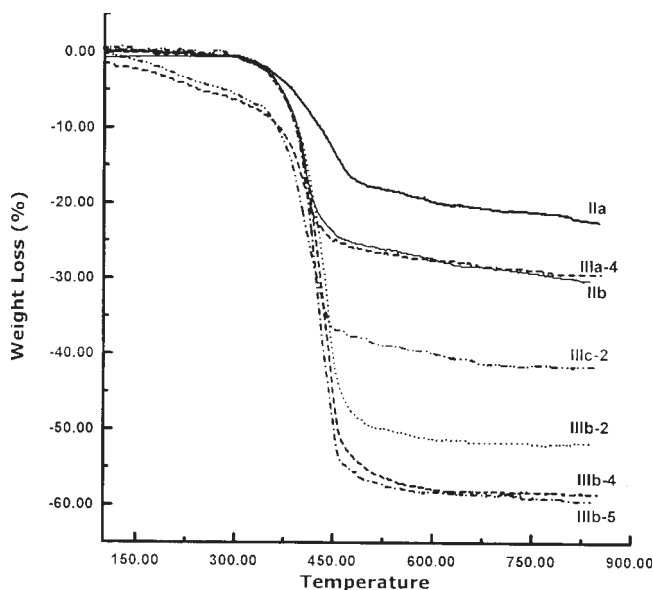**Scheme 3** Degradation of ammonium salts according to Hofmann elimination reaction.

clays has been reported to lose ammonia and give a proton counter ion.
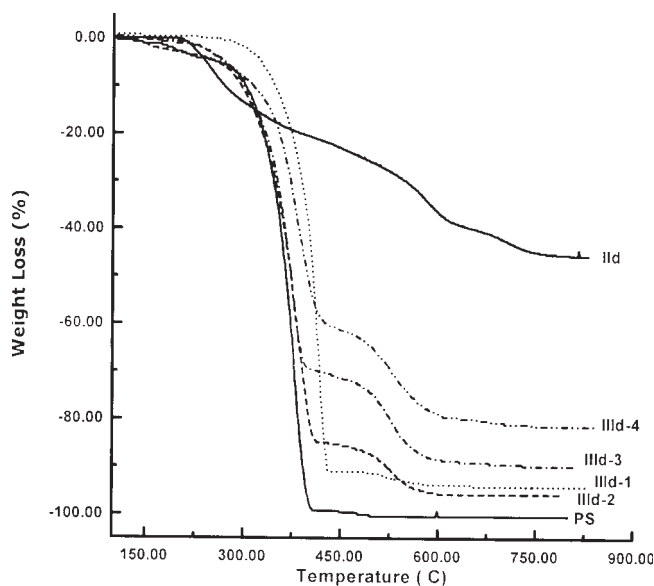
Thermal properties

The thermal stability of the prepared materials was determined by measuring the thermogravimetric analyses (TGA) within the temperature range of $\approx$ 30–850°C, as shown in Figures 7 and 8 and Table III. In general, the data and the figures indicated that the intercalated samples have higher thermal stability than the pure polymer. This can be attributed to the restriction of the motion of organic chains attached to the MMT clay.

The TGA data listed in Table III show the onset temperature of the degradation at which 5% and/or 10% degradation occurs is affected by the quaternary onium groups attached to the MMT clay. It was found that the degradation temperature is lower for materials attached through ammonium group compared with materials attached through phosphonium groups. It was also found that the amount of char was increased with increasing the clay contents. These results were correspond with those of Blumstein,[29] suggesting that the clay offers a templating effect.

Figure 7 shows that the thermal decomposition of some PS–MMT materials **III**a(c) takes place in one step

Figure 7 TGA thermograms of vinyl monomer–clay intercalates **II**a,b and some grafted PS–clay materials **III**a,c.

Figure 8 TGA thermograms of ungrafted PS, vinyl monomer–clay intercalate II_d and grafted PS–clay materials III_d.

occurred in the temperature range $\approx$ 280–410°C with weight loss ranged from 60 to 90 (wt %). This stage was attributed to the thermal decomposition of the PS on the surface and ungrafted PS in the interlayers of MMT. The second step of weight loss ranged from 10 to 20 wt %, takes place at the temperature range from $\approx$ 410–575°C due to the thermal decomposition of PS chains grafted to MMT and formation of black charred residues. The degradation rates of the nanocomposite samples in the second step are slower than the homo PS sample and the rates decrease with increasing the vinyl aliphatic chain content in the nanocomposite samples. This beneficial effect can illustrate the hindrances effect of grafted polystyrene on the MMT layer, which increases the interface between MMT and PS, which leads to the prevention of diffusion of oxygen and volatile products throughout the composite materials.

At 50% weight loss, the thermal decomposition temperatures of pure PS and PS–MMT III_d containing 5, 10, 20, and 40 wt % organoclay were determined as 369°, 407°, 372°, 372°, and 400°C, respectively. The data presented in Figure 8 illustrate that the clay contents play an effective reason for increasing the thermal properties of these materials. The PS–MMT $III_{d(1)}$ (containing wt-5% of organoclay) show higher thermal stability, which can be explained by the increasing homogeneous dispersion and the number of exfoliated individual layers, leading to the increased thermal stability of the material. It was found that the thermal decomposition temperature of PS–MMT $III_{d(1)}$, $III_{d(2)}$, and $III_{d(4)}$ was higher than pure PS with 43°, 8°, and 36°C, respectively. These results reflect the effect of clay contents on the increasing the thermal stability of the composite materials. Also, the thermal decomposition temperature of PS–MMT $III_{d(2)}$ and

starting from $\approx$ 360°C to $\approx$ 475°C with the remaining residual materials. But the thermal decomposition of linear PS sample occurs in one step and takes place completely in the range of $\approx$ 196–416°C. This may be due to the thermal decomposition of PS chains attached to MMT and formation of black charred residues.

Table III and Figure 8 depict the TGA curves of linear PS and grafted PS–MMT III_d with different clay contents. It was found that the thermal behavior of the PS–MMT nanocomposite was characterized by increasing the thermal properties in compared with the pure PS polymer. Also, the thermal decomposition was occurred in two stages: the first stage was

TABLE III
Thermal Analysis Data for Vinyl Monomer–Clay II_{a-d} and Some Grafted Polystyrene–Clay Composites

| Sample	TGA data						
	$T_{0.05}$	$T_{0.1}$	$T_{0.5}$	DTR			Char (%)
				Start	End	Wt loss (%)	
II_a	384	425	—	315	511	18	79
II_c	241	366	—	100	461	23	70
II_d	241	369	—	219	635	39	55
PS	262	302	364	196	416	100	0
$III_{a(4)}$	380	400	—	359	467	24	71
$III_{b(2)}$	364	391	502	356	494	49	49.5
$III_{b(3)}$	363	391	459	340	499	57	42
$III_{c(4)}$	360	385	449	342	496	56	40
$III_{c(2)}$	247	356	—	119	477	38	59
$III_{d(1)}$	325	347	407	379	449	91	6
$III_{d(2)}$	282	305	372	269	419, 575	91	8
$III_{d(3)}$	270	300	372	251	407, 585	88	10
$III_{d(4)}$	270	313	400	231	434, 595	78	19

DTR, degradation temperature range.

$III_{d(3)}$ nearly the same, this may be due to the use of insufficient solvent during preparation.

SEM and TEM results

The examination of the surface of the deposition-molded samples was followed by scanning electron microscopy (SEM). The SEM indicates that the PS was intercalated in the interlayer of MMT in a homogeneous manner to produce new polymer–MMT composite materials. The SEM does not show the MMT particles at the micron (μm) level. Figure 9 presents an SEM of the surface at different magnifications for the sample $III_{a(3)}$. The absence of MMT particles indicates that the agglomerate did not reveal the inorganic domains at the possible magnification. The particle size of MMT (0.1–10 μm) is not visible because it is well adherent to the polymer and the size of particle is below the resolution of

SEM. This indicates that the mineral domains are submicron and homogeneously dispersed in the polymer matrix. It also, indicates that the polymer was intercalated in the interlayer of MMT in a homogeneous manner to produce new PS–MMT nanocomposite materials.

The TEM of a thin film fabricated from acetone suspension of composite $III_{d(2)}$ is illustrated in Figure 10. The TEM shows that the PS–MMT intercalates have spherical particles in which the polymer is bound to the clay, homogeneously dispersed in the polymer matrix. The diameter of the spherical particles ranged within 150–400 nm, with an average size of 350 nm. This indicates that the composite is actually a mixture of homo-polystyrene and spherical particles with a good particle–matrix adhesion. A related morphology has been observed previously for polystyrene and poly(styrene-co-maleic anhydride) intercalated clay nanocomposites.[19,20,30]
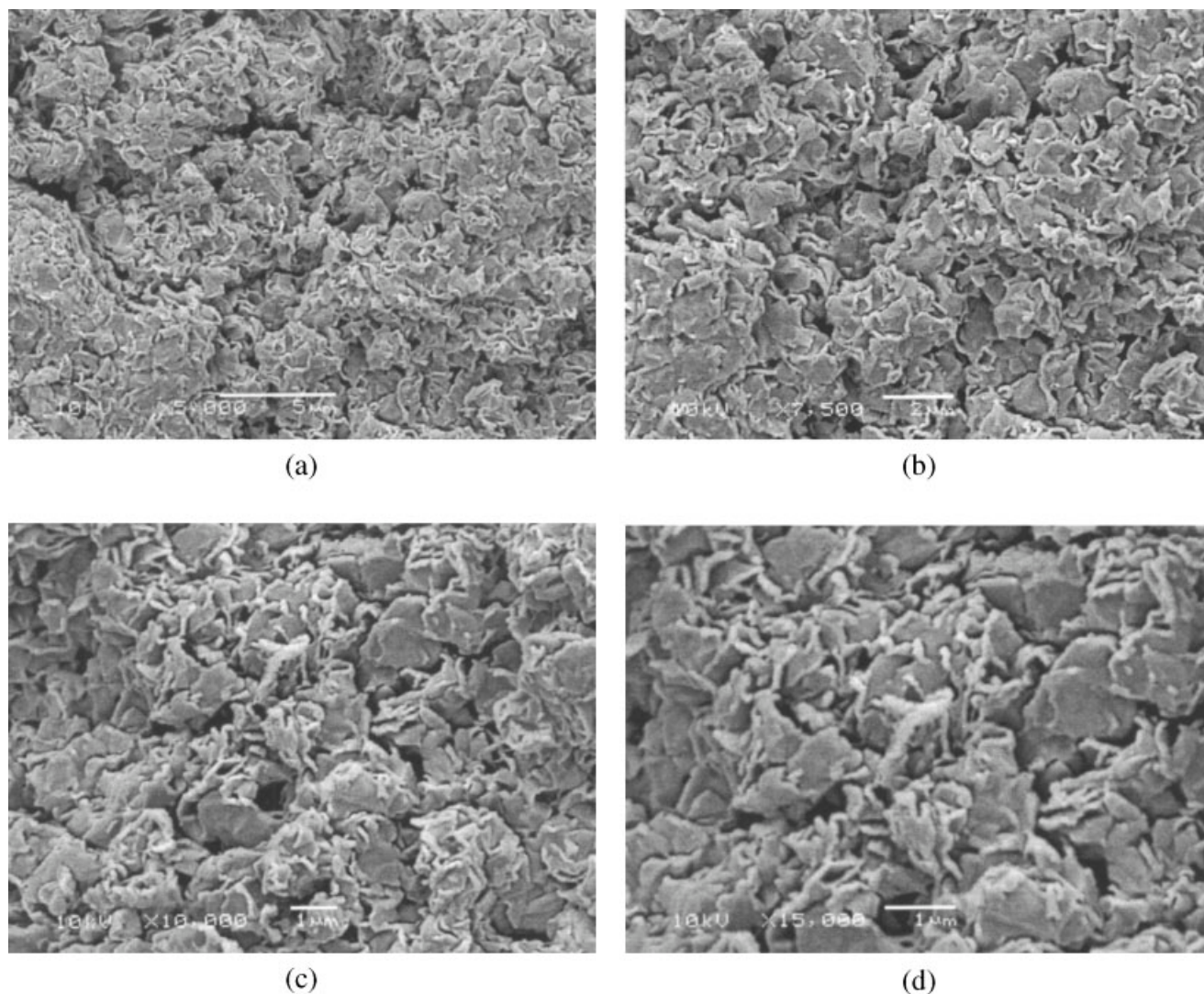
Figure 9   (a)–(d) SEMs of grafted PS–clay materials $III_{a(3)}$ at different magnifications.
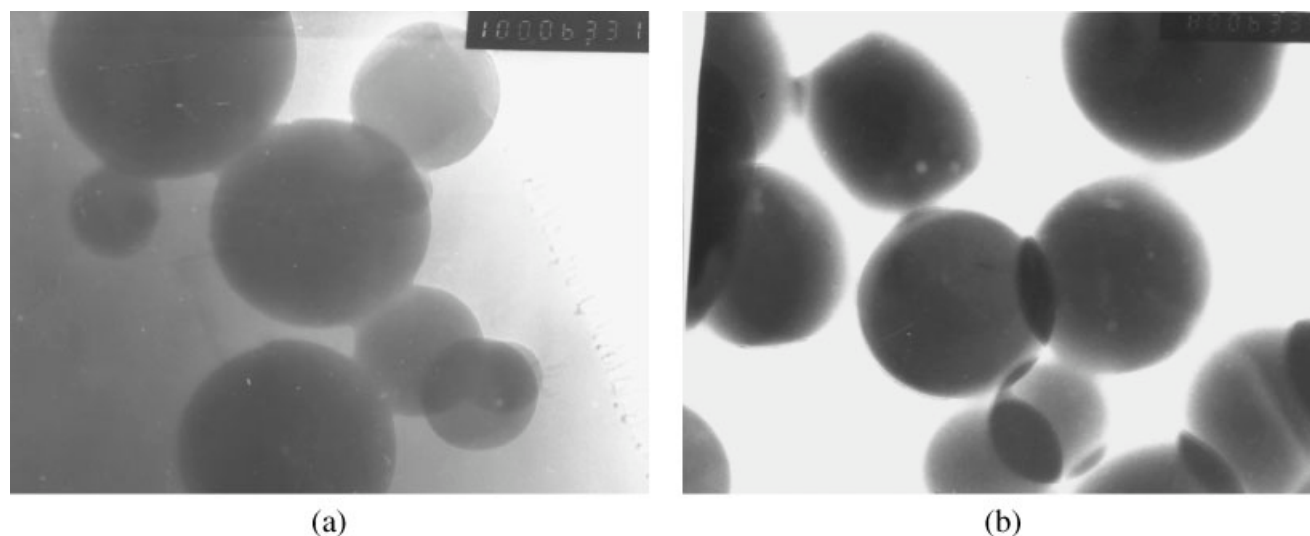
Figure 10 (a,b) TEM of grafted PS–clay material **III**$_{d(2)}$.

CONCLUSIONS

New polystyrene–organoclay nanocomposites have been prepared by grafting polymerization of styrene onto a vinyl monomer–MMT. The preparation was carried out by modification of the MMT with different vinyl monomers, such as *N,N*-dimethyl-*n*-octadecyl-4-vinylbenzyl-ammonium chloride, *n*-octadecyl-4-vinyl-benzyl-ammonium chloride, triphenyl-4-vinylbenzyl-phosphonium chloride, and tri-*n*-butyl-4-vinylbenzyl-phosphonium chloride; *in situ* polymerization of the styrene monomer with different ratios of vinyl mono-mer–MMT was then carried out.

The characteristic properties of the prepared materials were investigated by different physical and chemical analytical methods. Verification of the intercalation of the vinyl monomer–cation within the clay interlayers was achieved by IR spectra. The thermal properties were determined from the TGA, which exhibited higher thermal stability for PS–MMT nanocomposites than polystyrene (PS). Also, the TGA showed that formation of PS–MMT nanocomposites through phosphonium moieties between the MMT and polymer has higher thermal stability than the formation of PS–MMT nanocomposites through ammonium moieties. The swelling measurements in different organic solvents showed that the swelling degree in hydrophobic solvents increases as the clay ratio decreases. XRD analysis illustrates that the nanocomposites were exfoliated at ≤ 25 wt % of organoclay contents. SEM shows a complete dispersion of PS into the clay galleries. Also, TEM shows the formation of spherical particles within a nanosize range of 150–400 nm.

References

1. Novak, B. M. Adv Mater 1993, 5, 422.
2. Wang, S.; Long, C.; Wang, X.; Li, Q.; Qi, Z. J Appl Polym Sci 1998, 69, 1557.
3. Usuki, A.; Kawasumi, M.; Kojima, Y.; Okada, A.; Kurauchi, T.; Kamingato, O. J Mater Res 1993, 8, 1179, 1185.
4. Wang, M. S.; Pinnavaia, T. J. Chem Mater 1994, 6, 468.
5. Sharp, K. G. Adv. Mater 1998, 10, 1243.
6. Bumside, S. D.; Wang, H.; Giannelis, E. P. Chem Mater 1999, 11, 1055.
7. Noh, M. W.; Lee, D. C. Polym Bull 1999, 42, 619.
8. Zhu, J.; Wilkie, C. A. Polym Inter 2000, 49, 1158.
9. Vaia, R. A.; Giannelis, E. P. Macromoleules 1997, 30, 8000.
10. Liu, L. M.; Qi, Z. N.; Zhu, X. G. J Appl Polym Sci 1999, 61, 1117.
11. Carrado, K. A.; Xu, L. Q. Chem Mater 1998, 10, 1440.
12. Yeh, J.-M.; Liou, S.-J.; Lai, C.-Y.; Wu, P.-C. Chem Mater 2002, 14, 154.
13. Wang, D.; Zhu, J.; Yao, Q.; Wilkie, C. A. Chem Mater 2002, 14, 3837.
14. Hackett, E.; Manias, E.; Giannelis, E. P. J Chem Phys 1998, 108, 7410.
15. Claudia, F.; Marco, G.; Silvia, G.; Giacomo, R.; Carlo, A. V.; Bernardo, M. Polymer 1998, 39, 2651.
16. Sugahara, Y.; Satokawa, S.; Kuroda, K.; Kato, C. Clays Clay Miner 1998, 36, 343.
17. Salahuddin, N.; Rehab, A. Polym Internat 2003, 52, 241.
18. Kato, C.; Kuroda, K.; Takahara, H. Clays Clay Miner 1981, 29, 294.
19. Akelah, A.; Moet, A. J Mater Sci 1996, 31, 3589.
20. Moet, A.; Akelah, A. Mater Lett 1993, 18, 97.
21. Akelah, A.; Rehab, A.; Selim, A.; Agag, T. J Mol Cat 1994, 94, 311.
22. Doh, J. G.; Cho, I. Polym Bull 1998, 41, 511.
23. Fu, X.; Qutubuddin, S. Polymer 2001, 42, 807.
24. Tseng, C. -R.; Wu, J. -Y.; Lee, H. -Y.; Chang, F.-C. J Appl Polym Sci 2002, 85, 1370.
25. Rehab, A.; Akelah, A.; Agag, T.; Betiha, M. J Appl Polym Sci 2006, submitted.
26. Grim, R. E. Clay Mineralogy; McGraw-Hill: New York, 1968.
27. Xie, W.; Gao, Z.; Pan, W. P.; Vaia, R.; Hunter, D.; Singh, A. Polym Mater Sci Eng. 2000, 83, 284.
28. Jones, M. Organic Chemistry, 2nd ed; WW Norton: New York, 2000; p 258.
29. Blumstein, A. J Polym Sci Part A 1965, 3, 2653.
30. Salhuddin, N.; Akelah, A. Polym Adv Technol 2002, 13, 339.